MNRAS **000**, 000–000 (0000) Preprint 15 June 2016 Compiled using MNRAS LaTeX style file v3.0

Resonant Barriers and Resonant escape: why high inclination KBOs are preferentially captured as Neptune Trojans

order and author list to be determined,
Yuan-Yuan Chen[1], and ? and Alice C. Quillen[2], ...?
[1] *Key Laboratory of Planetary Sciences, Purple Mountain Observatory, Chinese Academy of Sciences, Nanjing 210008, China*
[2] *Department of Physics and Astronomy, University of Rochester, Rochester, NY 14627 USA*

15 June 2016

ABSTRACT
We contrast high inclination bodies captured into corotation resonances with Neptune during migration with low inclination bodies.

1 INTRODUCTION

A number of mechanisms have been proposed for capture of objects (Trojans) into corotation or 1:1 resonance with a giant planet or orbits orbiting the L4 or L5 (or both) Lagrange points (for a review see Marzari et al. 2002). The capture efficiency is highest (up to 50%) for a capture scenario where nearby planetesimals are captured into resonance as the planet becomes more massive as the resonance widens and strengthens (e.g., Fleming & Hamilton 2000; Marzari & Scholl 1998). Once trapped as a Trojan, the libration amplitude of a planetesimal continues to shrink under the influence of the growing Jupiter. We must keep in mind that long term stability must be considered after capture.

Chaotic capture: The capture of Jupiter Trojans in the Nice model occurs during discrete episodes when the coorbital region is swept by secondary resonances associated with mean-motion commensurabilities between Jupiter and Saturn Morbidelli et al. (2005); Marzari & Scholl (2007); Robutel & Bodossian (2009); Nesvorny & Vokrouhlicky (2009). This process, called chaotic capture, might explain how Neptune acquired its Trojans via resonances between Uranus and Neptune (Nesvorny & Vokrouhlicky 2009) as Neptune and Uranus migrated. Recent numerical simulations of Neptune's migration through a primordial disk have shown that high inclination objects are preferentially captured and retained as Trojans (Parker 2015; Chen et al. 2016).

After capture into corotation resonance, planet migration can cause objects to escape the corotation resonance. Kortenkamp et al. (2004) showed that Trojan particles escape the corotation region when they are swept by secondary resonances associated with mean-motion commensurabilities of Uranus with Neptune. These secondary resonances arise when the circulation frequencies, of critical arguments for Uranus and Neptune mean-motion near-resonances are commensurate with harmonics of the libration frequency of the critical argument for the Neptune-Trojan 1:1 mean- motion resonance. As these resonances involve three bodies, the Trojan, Neptune and Uranus they can also be called three-body resonances.

2 THREE BODY RESONANCES

We first make an approximate model for libration of Trojan type objects in the corotation region of an outer planet. We then consider how an external planet is perturbed due to a mean motion resonance with an internal planet. We then modify the libration model to take into account the induced perturbations of the outer planet. The model is a three-body resonance model (e.g., Murray et al. 1998; Nesvorný & Morbidelli 1998a; Quillen 2011; Quillen & French 2014). In this case the corotating Trojan object is perturbed by Neptune which is perturbed by resonance with Uranus. Our goal is to understand why lower inclination objects might preferentially escape the corotation region. With an estimate of the strength of the three-body resonances we can determine the likelihood that a drifting system (Uranus migrating with respect to Neptune) will allow capture of a Trojan into the three-body resonance (employing the order of magnitude approach by Quillen 2006).

2.1 Libration near corotation

We first consider an approximate model for libration about an L4 or L5 Lagrange point following the framework given by Tabachnik & Evans (2000) (see their section 2). We work in Poincaré coordinates and consider the restricted problem of three bodies (Sun, planet and planetesimal). The Hamiltonian in a non-rotating heliocentric frame for the asteroid

$$H = -\frac{k^2}{2a} - m_p k^2 R \tag{1}$$

where k is the Gaussian gravitational constant, a is the asteroid's semi-major axis, m_p is the mass of the planet in solar masses and R is the disturbing function. Setting units so that $k = 1$ and in Poincaré coordinates (the conjugate momenta and angles)

$$H(\Lambda, \Gamma, Z; \lambda, \gamma, z) = -\frac{1}{2\Lambda^2} - m_p R \tag{2}$$

Here Poincaré angles $\gamma = \Omega + \omega = -\varpi$ and $z = -\Omega$ with Ω the longitude of the ascending node and ω is argument of pericenter and ϖ is the longitude of pericenter. The momenta $\Gamma = \sqrt{a}$, $\Gamma \approx \sqrt{a}e^2/2$ and $Z \approx \sqrt{a}(1 - \cos i)$ with e and i the eccentricity and inclination of the planetesimal. The disturbing function depends on the momenta and angles as well as the coordinates of the planet. The semi-major axis for corotation $a = a_p$ with a_p the semi-major axis of the planet. Hereafter quantities subscripted with p refer to the planet. Expanding near corotation $\Lambda = \Lambda_p + l$ with $\Lambda_p = \sqrt{a_p}$

$$H(l, \Gamma, Z; \lambda, \gamma, z) \approx -\frac{1}{2\Lambda_p^2} + \frac{l}{\Lambda_p^3} - \frac{3}{2}\frac{l^2}{\Lambda_p^4} - m_p R \tag{3}$$

The disturbing function can be expanded in orders of eccentricity and inclination of asteroid and planet. It can also be expanded in Fourier components of angles. Often it is helpful to consider a model where only some Fourier components (those with slowly varying angles) are retained. An alternative approach is to average over a fast angle. Tabachnik & Evans (2000) averages the disturbing function over the planet's mean anomaly, M_p, $\langle R \rangle = \int_0^{2\pi} R dM_p$ (see their equation 4). The resulting averaged disturbing function shows minima near $\phi_* \sim \pm\pi/3$, the L4 and L5 Lagrange points, as expected (see their Figure 2 and Figure 1) where $\phi \equiv \lambda - \lambda_p$ and λ and λ_p are the mean longitudes of asteroid and planet.

2.2 Fourier coefficients of the averaged disturbing function near corotation

Tabachnik & Evans (2000) show an a second order expansion of the averaged disturbing function. The zero-th order (in eccentricity) term is

$$U_0 = (a^2 + a_p^2 - 2aa_p \cos^2 \tfrac{i}{2} \cos\phi)^{-\frac{1}{2}} - \frac{a}{a_p^2} \cos^2 \tfrac{i}{2} \cos\phi \tag{4}$$

(equation by Tabachnik & Evans 2000). In Figure 1 we plot $U(\phi)$ for $a = a_p = 1$ and for $i = 1°$ and $i = 40°$. The shape is similar to that shown in Figure 2 by Tabachnik & Evans (2000) and has the characteristic two minima for L4 and L5 Lagrange points.

We expand the averaged disturbing function in Fourier components

$$\langle R \rangle(\phi) = \sum_m b_m \cos(n\phi) \tag{5}$$

We see from Figure 1 that the zero-th order term of the averaged disturbing function has a steeper slope near $\phi = 0$ at lower inclination than at higher inclination. This follows as the first term in equation 4 has a discontinuity at $\phi = 0$ at zero inclination, corresponding to a close approach of particle and planet. The steeper slope for U_0 implies that that high m Fourier coefficients are stronger at low inclination than at high inclination.

We numerically compute the Fourier components of U_0 for inclinations $i = 1, 5, 10, 20, 30, 40°$ and they are plotted on a log scale as a function of m in Figure 2 for $a = a_p = 1$.

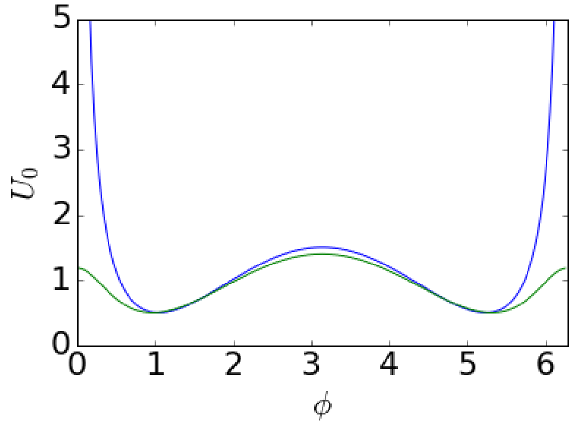

Figure 1. The zero-th order term of the disturbing function U_0 plotted for inclinations $i = 1°$ in blue and $i = 40°$ in green.

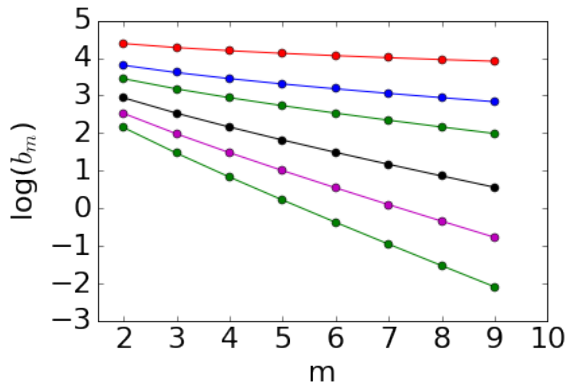

Figure 2. The Fourier components of U_0 for $a = a_p = 1$ are plotted as a function of Fourier index m. We plot $\log b_m$, the cosine amplitude for (from top to bottom) inclinations $i = 1, 5, 10, 20, 30, 40°$. The strength of the component decays exponentially with m and the decay rate is faster at higher inclination.

The reflection symmetry of U_0 implies that we need only consider the cosine amplitudes (the sine coefficients vanish). Figure 2 shows that the Fourier components decay exponentially and faster (with m) at higher inclination. To a good approximation

$$b_m \propto e^{-s_b m} \tag{6}$$

with slope $s_b(i)$. The exponential form and rate of decay is likely related to the width of analytical continuation in the complex plane of the function U_0 (see Quillen 2011 on approximating Laplace coefficients).

From the points plotted in Figure 2 and for each inclination we fit a slope $s_b(i)$ assuming equation 6. The measured slopes are plotted as a function of inclination in Figure 3. We find that the slopes are well approximated by $s_b \approx 0.76i$ with inclination i in radians.

We have estimated the decay rate of the Fourier coefficients of the averaged disturbing function using the zero-th order term U_0 finding cosine coefficients $b_m \propto e^{-s_b m}$ with $s_b(i) = 0.76i$. Hereafter we assume that the same exponential scaling holds for the entire averaged disturbing function.

In Figure 4 we plot b_2 as a function of inclination, again

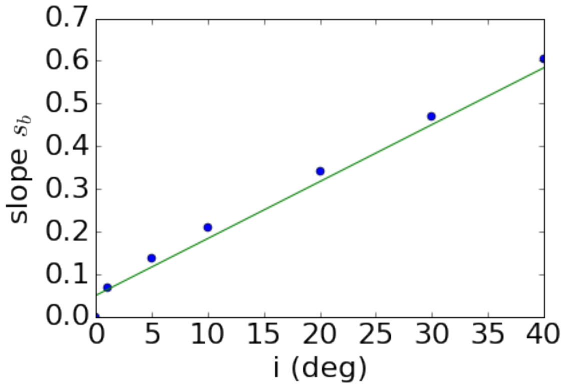

Figure 3. The slopes s_b measured from the points in Figure 2 are plotted as a function of inclination along with a linear fit.

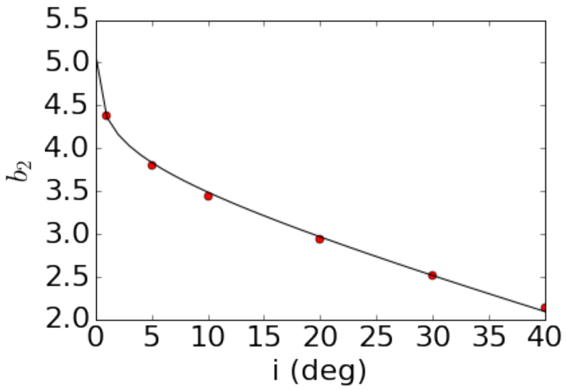

Figure 4. The $m = 2$ Fourier coefficient, b_2 measured from U_0 as a function of inclination, shown as points, with a line given by equation 7

measured from U_0. A reasonable fit to this is shown as a black like on the plot and is given by

$$b_m(i) \sim 30 i^{\frac{1}{4}} e^{-mi} \tag{7}$$

Inserting this function into the Hamiltonian in equation 3 gives us an approximate model for libration that includes the high m Fourier coefficients;

$$\begin{aligned} H(l,\Gamma,Z;\lambda,\gamma,z) \quad \approx \quad & \frac{l}{\Lambda_p^3} - \frac{3}{2}\frac{l^2}{\Lambda_p^4} \\ & - \frac{m_p}{a_p} 30 i^{\frac{1}{4}} \sum_m e^{-mi}\cos(m(\lambda-\lambda_p)) \end{aligned} \tag{8}$$

where we have dropped the constant term. We did approximations using $a = a_p$ and we have restored an estimate for the dependence on a_p using the first term in U_0 that likely controls the exponential decay of the high m Fourier coefficients. We have checked that the exponential scaling $b_m \propto e^{-mi}$ holds for the the derivative of U_0 with respect to a.

3 PERTURBATION OF NEPTUNE BY URANUS NEAR 2:1 MEAN MOTION RESONANCE

Following Murray & Dermott (1999) section 6.9.2 but for an internal perturber the relevant part of the averaged disturbing function for the 2:1 mean motion resonance contains two terms

$$R = \frac{m_U}{a_N}\left[C_4 e_U \cos(2\lambda_N - \lambda_U - \varpi_U)\right. \tag{9}$$

$$\left. +(C_5 - \tfrac{1}{2})\frac{a_N^2}{a_U^2} e_N \cos(2\lambda_N - \lambda_U - \varpi_N)\right] \tag{10}$$

with

$$C_4 \quad = \quad \tfrac{1}{2}\left[-4 - \alpha D\right] b_{\frac{1}{2}}^{(2)}(\alpha) \tag{11}$$

$$C_5 \quad = \quad \tfrac{1}{2}\left[3 + \alpha D\right] b_{\frac{1}{2}}^{(1)}(\alpha) \tag{12}$$

using $q = 2$ and f_{27} and f_{31} in appendix of M+D and $\alpha_{UN} = a_U/a_N$ near the 2:1 resonance and $b_{\frac{1}{2}}^{(2)}$ a Laplace coefficient. Here $D \equiv \frac{d}{d\alpha}$

Lagrange's equation for $\dot{a}_N$ give

$$\begin{aligned} \dot{a}_N = & \quad \frac{2}{n_N a_N}\frac{\partial R}{\partial \lambda_N} \\ = & \quad -\frac{4 m_U}{n_N a_N^2}\left[C_4 e_U \sin\phi_U + (C5 - \tfrac{1}{2\alpha^2}) e_N \sin\phi_N\right] \end{aligned} \tag{13}$$

using shorthand

$$\begin{aligned} \phi_U &\equiv 2\lambda_N - \lambda_U - \varpi_U \\ \phi_N &\equiv 2\lambda_N - \lambda_U - \varpi_N . \end{aligned} \tag{14}$$

Integrating this we find excursions in semi-major axis from the resonance

$$\begin{aligned} \Delta a_N \quad \sim & \quad \frac{4 m_U}{n_N a_N^2}\left[\frac{C_4 e_U}{2n_N - n_U - \dot\varpi_U}\cos\phi_U\right. \\ & \left. +(C_5 - \tfrac{1}{2\alpha^2})\frac{e_N}{2n_N - n_U - \dot\varpi_U}\cos\phi_N\right] \end{aligned} \tag{15}$$

Lagrange's equation for $\dot\lambda_N$ give

$$\begin{aligned} \dot\lambda_N \quad = & \quad -\frac{2}{n_N a_N}\frac{\partial R}{\partial a_N} \\ = & \quad -\frac{2 m_U}{n_N a_N^3}\left[(1+\alpha D) C_4 e_U \cos\phi_U\right. \\ & \quad \left. + \left((1+\alpha D) C_5 + \tfrac{1}{2\alpha^2}\right) e_N \cos\phi_N\right] \end{aligned} \tag{16}$$

Integrating this we get an excursion in mean longitude due to resonance

$$\begin{aligned} \Delta\lambda_N \quad \sim & \quad -\frac{2 m_U}{n_N a_N^3}\left[\frac{(1+\alpha D) C_4}{2n_N - n_U - \dot\varpi_U} e_U \sin\phi_U\right. \\ & \left. + \frac{(1+\alpha D) C_5 + (2\alpha^2)^{-1}}{2n_N - n_U - \dot\varpi_N} e_N \sin\phi_N\right] \end{aligned} \tag{17}$$

Evaluating coefficients near the 2:1 resonance

$$C_4 \quad = \quad -1.2 \tag{18}$$

$$C_5 \quad = \quad 1.7 \tag{19}$$

$$C_{5x} \quad = \quad (C_5 - \tfrac{1}{2})\frac{a_N^2}{a_U^2} = 0.4 \tag{20}$$

$$C_{4y} \quad = \quad (1+\alpha D) C_4 = -4.5 \tag{21}$$

$$C_{5y} \quad = \quad (1+\alpha D) C_5 + (2\alpha^2)^{-1} = 6.0 \tag{22}$$

The only one of these that is extremely sensitive to semi-major axis ratio is the third one, C_{5x}. For $\alpha = 0.6$ it is only $C_{5x} = 0.16$ whereas for $\alpha = 0.65$ it is $C_{5x} = 0.6$.

Defining

$$A_U \equiv \frac{4m_U}{n_N a_N^2}\frac{C_4 e_U}{2n_N - n_U - \dot\varpi_U} \quad (23)$$

$$A_N \equiv \frac{4m_U}{n_N a_N^2}\frac{4C_{5x} e_N}{2n_N - n_U - \dot\varpi_N} \quad (24)$$

$$B_U \equiv -\frac{2m_U}{n_N a_N^3}\frac{C_{4y} e_U}{2n_N - n_U - \dot\varpi_U} \quad (25)$$

$$B_N \equiv -\frac{2m_U}{n_N a_N^3}\frac{C_{5y} e_N}{2n_N - n_U - \dot\varpi_N} \quad (26)$$

$$(27)$$

equations 15 and 17 are written

$$\Delta\lambda_N \sim A_U \cos(2\lambda_N - \lambda_U - \varpi_U) + A_N \cos(2\lambda_N - \lambda_U - \varpi_N) \quad (28)$$

$$\Delta a_N \sim B_U \sin(2\lambda_N - \lambda_U - \varpi_U) + B_N \sin(2\lambda_N - \lambda_U - \varpi_N) \quad (29)$$

3.1 Three body resonance

We recall equation 8 here but replacing a_p with a_N and similarly for other elements

$$H(l,\Gamma,Z;\lambda,\gamma,z) \approx \frac{l}{\Lambda_p^3} - \frac{3}{2}\frac{l^2}{\Lambda_N^4} - \frac{m_N}{a_N} 30 i^{\frac{1}{4}} \sum_m e^{-mi}\cos(m(\lambda-\lambda_N)) \quad (30)$$

We insert $a_N = a_{N0} + \Delta a_N$ and $\lambda_N = n_N t + \Delta\lambda_{N0} + \Delta\lambda_N$ into the last term, retaining first order terms

$$x = \frac{m_N}{a_{N0}^2}\Delta a_N 30 i^{\frac{1}{4}} \textstyle\sum_m e^{-mi}\cos(m(\lambda-\lambda_N))$$

$$+\frac{m_N}{a_N} 30 i^{\frac{1}{4}} \textstyle\sum_m e^{-mi}\sin(m(\lambda-\lambda_N)) m\Delta\lambda_N \quad (31)$$

$$= \frac{m_N}{a_N 0} 30 i^{\frac{1}{4}} \textstyle\sum_m e^{mi} \quad (32)$$

We retain only first order terms so close!

4 MEAN MOTION RESONANCE BETWEEN TWO PLANETS

Because both planets have mass we must use Poincaré coordinates including the body masses. For planet with index i, the momentum $\Lambda_i = m_i\sqrt{a_i}$ and similarly for $\Gamma_i \approx m_i\sqrt{a_i}e_i^2/2$ and Z_i. The Hamiltonian is

$$H = -\frac{m_i^3}{2\Lambda_i^2} - \frac{m_j^3}{2\Lambda_j^2} + R_{ij} \quad (33)$$

where R_{ij} is the disturbing function coming from the gravitational interaction between planets.

A first order $q-1:q$ mean motion resonance between two planets can be modeled with Fourier components from the low eccentricity expansion of the disturbing function (following equation 32-34 by Quillen & French 2014)

$$V^i\cos(q\lambda_j + (1-q)\lambda_i - \varpi_i) + V^j\cos(q\lambda_j + (1-q)\lambda_i - \varpi_j) \quad (34)$$

with

$$V^i = -\frac{m_i m_j}{a_j} e_i f_{27}(\alpha_{ij},q) \approx -\frac{m_i m_j^3}{\Lambda_j^2}\left(\frac{2\Gamma_i}{\Lambda_i}\right)^{\frac{1}{2}} f_{27}(\alpha_{ij},q)$$

$$V^j = -\frac{m_i m_j}{a_j} e_j f_{31}(\alpha_{ij},q) \approx -\frac{m_i m_j^3}{\Lambda_j^2}\left(\frac{2\Gamma_j}{\Lambda_j}\right)^{\frac{1}{2}} f_{31}(\alpha_{ij},q) \quad (35)$$

with $\alpha_{ij} = a_i/a_j$ and we assume that $a_i < a_j$. We are primarily interested in how the resonance causes perturbations to the mean longitude of the outer planet, here λ_j (as equation 8 contains an angle which depends on λ_p).

Taking derivatives of the Fourier components (of the disturbing function)

$$\dot\lambda_j = \frac{\partial H}{\partial\Lambda_j} = n_j + \frac{\partial V^i}{\partial\Lambda_j}\cos\phi_i + \frac{\partial V^j}{\partial\Lambda_j}\cos\phi_j \quad (36)$$

with $\phi_i = q\lambda_j + (1-q)\lambda_i - \varpi_i$ and $\phi_i = q\lambda_j + (1-q)\lambda_i - \varpi_j$.

$$\frac{\partial V^i}{\partial\Lambda_j} = \frac{m_i m_j^3}{\Lambda_j^2}\left(\frac{2\Gamma_i}{\Lambda_i}\right)^{\frac{1}{2}} 2\left[\frac{f_{27}}{\Lambda_j} + f_{27}'\frac{\Lambda_i^2}{\Lambda_j^3}\right] \quad (37)$$

$$= m_i n_j 2 e_i\left[f_{27} + f_{27}'\frac{m_i^2}{m_j^2}\alpha_{ij}\right] \quad (38)$$

$$\frac{\partial V^j}{\partial\Lambda_j} = \frac{m_i m_j^3}{\Lambda_j^2}\left(\frac{2\Gamma_j}{\Lambda_j}\right)^{\frac{1}{2}}\left[\frac{5}{2}\frac{f_{31}}{\Lambda_j} + 2f_{31}'\frac{\Lambda_i^2}{\Lambda_j^3}\right] \quad (39)$$

$$= m_i n_j e_j\left[\frac{5}{2}f_{31} + 2f_{31}'\frac{m_i^2}{m_j^2}\alpha_{ij}\right] \quad (40)$$

We can integrate 36 to estimate

$$\lambda_j = n_j t + (qn_j + (1-q)n_i)^{-1}\left[\frac{\partial V^i}{\partial\Lambda_j}\sin\phi_j + \frac{\partial V^j}{\partial\Lambda_j}\sin\phi_j\right] \quad (41)$$

For short we will refer to

$$\epsilon_i = (qn_j + (1-q)n_i)^{-1}\frac{\partial V^i}{\partial\Lambda_j} \quad (42)$$

$$\epsilon_j = (qn_j + (1-q)n_i)^{-1}\frac{\partial V^j}{\partial\Lambda_j} \quad (43)$$

giving

$$\lambda_j = \lambda_0 + \epsilon_i\sin\phi_i + \epsilon_j\sin\phi_j \quad (44)$$

with $\lambda_0 = n_j t$. We expect the two perturbation strengths ϵ_i, ϵ_j are not large.

We will use the terms proportional to $\sin\phi_i$ and $\sin\phi_j$ to construct a three-body resonance using equation 8.

We need to add indirect term for 2:1 resonance

4.1 Three body resonance

Substituting into equation 8 using $\lambda_j = \lambda_p$. We consider argument

$$\cos(2(\lambda-\lambda_p)) \approx \cos(2(\lambda-\lambda_0)) + \sin(2(\lambda-\lambda_0))(2\epsilon_i\sin\phi_i + 2\epsilon_j\sin\phi_j) \ ($$

Picking up resonant arguments that look like this

$$\epsilon_i\cos(2(\lambda-\lambda_p)\pm\phi_i) + \epsilon_j\cos(2(\lambda-\lambda_p)\pm\phi_j) \quad (46)$$

Putting back into Hamiltonian the three body resonance looks like this

$$H = l^2 + \omega_{lib}^2\epsilon_i\cos(2(\lambda-\lambda_p)\pm\phi_i) + \epsilon_j\cos(2(\lambda-\lambda_p)\pm\phi_j) \quad (47)$$

The frequency of the ith three body resonance is

$$\omega_3 \sim \omega_{lib}\sqrt{\epsilon_i}$$

Note We used only λ_p but actually the libration frequency depends on a_p also and that is varying during resonance. We can neglect eccentricity e_p and ϖ_p variations probably.

4.2 What?

The width and libration amplitude in 1:1 resonance are somewhat sensitive to inclination (as shown in expansion;Tabachnik & Evans 2000) and as shown by the sensitivity of libration frequency to orbital inclination (Zhou et al. 2011). Zhou et al. (2011) measured a libration frequency of 1.13, 1.01, 0.88 for inclinations of $5, 35, 55^\circ$ respectively, in units of $10^{-4} 2\pi \text{yr}^{-1}$ (see their equations 1, 8, 13, for zero eccentricity and with semi-major axis in the center of the corotation resonance).

Zhou et al. (2011) uses $f_{2:1} = 2\lambda_N - \lambda_U$. We might want to define $\phi_{2:1} = 2\lambda_N - \lambda_U - \varpi_x$ Which body? It's not necessarily the one you think because of the cancellation by the indirect term!

Resonances in the form $j f_\sigma \sim k\phi_{2:1}$ with integers j, k, are probably important, (Kortenkamp et al. 2004) (and are in the class called C type by Zhou et al. 2011). To satisfy a d'Alembert rule additional factors of secular precession frequencies must be added (see equation 5 are associated discussion by Zhou et al. 2011).

These resonances can be considered 3-body resonances because they involve an angle constructed from xxx

REFERENCES

Chen; Y.-Y., Yuehua, Ma, Y., & Zheng, J. 2016, MNRAS, 458, 4277, The effect of orbital damping during planet migration on the inclination and eccentricity distributions of Neptunian Trojans

Deck, K. M., Holman, M. J., Agol, E., Carter, J. A., Lissauer, J. J., Ragozzine, D., & Winn, J. N. 2012, ApJ, 755, L21

Fleming, H. J., & Hamilton, D. P. 2000, Icarus, 148, 479 On the Origin of the Trojan Asteroids: Effects of Jupiter's Mass Accretion and Radial Migration

Kortenkamp, S. J., Malhotra, R., & Michtchenko, T. 2004, Icarus, 167, 347-359 Survival of Trojan-type companions of Neptune during primordial planet migration

Kortenkamp, S. J., & Joseph, E. C. S. 2011, Icarus, 215, 669-681. Transformation of Trojans into quasi-satellites during planetary migration and their subsequent close-encounters with the host planet

Lykawka, P. S., & Horner, J. 2010, MNRAS , 405, 1375, The capture of Trojan asteroids by the giant planets during planetary migration

Malhotra R., 1990, Icarus, 87, 249

Marzari F., Scholl, H., Murray, C., & Lagerkvist, C. 2002, Origin and Evolution of Trojan Asteroids, in Asteroids III, edited by William F. Bottke Jr.; Alberto Cellino; Paolo Paolicchi; Richard P. Binzel, pp. 725-738.

Marzari, F., & Scholl, H. 1998, Icarus, 131, 41-51 Capture of Trojans by a Growing Proto-Jupiter

Marzari, F., & Scholl, H. 2007, MNRAS, 380, 479 Dynamics of Jupiter Trojans during the 2:1 mean motion resonance crossing of Jupiter and Saturn

Morbidelli, A., Levison, H. F., Tsiganis, K., & Gomes, R. 2005, Nature, 435, 462-465 Chaotic capture of Jupiter's Trojan asteroids in the early Solar System.

Murray, C. D. & Dermott, S. F. 1999, Solar System Dynamics, Cambridge University Press, Cambridge

Murray, N., Holman, M., & Potter, M., 1998, *On the Origin of Chaos in the Asteroid Belt*, Astron. J., 116, 2583-2589.

Mustill, A. & Wyatt, M. C. 2011, MNRAS, 413, 554

Nesvorný, D., & Morbidelli, A. 1998, *An Analytic Model of Three-Body Mean Motion Resonances*, Celestial Mechanics and Dynamical Astronomy, 71, 243

Nesvorny, D., & Vokrouhlicky, D., 2009, AJ, 137, 5003-5011 Chaotic capture of Neptune Trojans.

Parker, A. H. 2015, Icarus, 247, 112 The intrinsic Neptune Trojan orbit distribution: Implications for the primordial disk and planet migration

Quillen, A. C., 2006, Reducing the probability of capture into resonance, MNRAS, 365, 1367-1382.

Quillen, A. C. 2011, MNRAS, 418, 1043

Quillen, A. C. & French, R. S. 2014, MNRAS, 445, 3959, Resonant chains and three-body resonances in the closely packed inner Uranian satellite system

Robutel, P., & Bodossian, J. 2009, MNRAS, 399, 69 The resonant structure of Jupiter's Trojan asteroids - II. What happens for different configurations of the planetary system

Tabachnik, S. A., & Evans, N. W. 2000, MNRAS, 319, 63, Asteroids in the inner Solar system - I. Existence

Tsiganis, K., Varvoglis, H., & Dvorak, R. 2005, CeMDA, 92, 71 Chaotic Diffusion And Effective Stability of Jupiter Trojans

Zhou, L.Y., Dvorak, R. , & Sun, Y.-S. 2011, MNRAS, 410, 1849?1860 The dynamics of Neptune Trojans ? II. Eccentric orbits and observed objects